

NUMERICAL MODEL FOR THE WEAKLY NONLINEAR PROPAGATION OF SOUND THROUGH TURBULENCE

55-71

29/62

p. 20

Bart Lipkens and Philippe Blanc-Benon
Laboratoire de Mécanique des Fluides et Acoustique
URA-CNRS 263
Ecole Centrale de Lyon
Ecully, France

INTRODUCTION

When finite amplitude (or intense) sound, such as a sonic boom, propagates through a turbulent atmosphere, the propagation is strongly affected by the turbulence. The interaction between sound and turbulence has mostly been studied as a linear phenomenon, i.e., the nonlinear behavior of the intense sound has been neglected. It has been shown that turbulence has an effect on the perceived loudness of sonic booms, mainly by changing its peak pressure and rise time. Peak pressure and rise time are important factors that determine the loudness of the sonic boom when heard outdoors [1, 2]. However, the interaction between turbulence and nonlinear effects has mostly not been included in propagation studies of sonic booms. It is therefore important to investigate the influence of acoustical nonlinearity on the interaction of intense sound with turbulence.

OVERVIEW

As stated in the introduction, the motivation for the research presented here is an investigation of the effect of turbulence on the nonlinear propagation of sonic booms and spark-produced N waves. In a previous study [2] Lipkens showed that model experiments are successful in simulating the sonic boom propagation through a turbulent atmosphere. A nonlinear propagation model for the propagation of sound through turbulence is presented here. Results from a numerical experiment that simulates the propagation of spark-produced N waves through turbulence are shown. Finally, some conclusions of the effect of turbulence on the nonlinear propagation of N waves are given.

Overview

- Motivation: study the effect of turbulence on the nonlinear propagation of sonic booms (N waves)
- Model experiment is successful in simulating the sonic boom propagation through atmospheric turbulence
- Nonlinear propagation model
- Results
- Conclusion

Figure 1: Overview of presentation.

MODEL EXPERIMENT

In Fig. 2 the setup of the model experiment is shown. The discharge of a capacitor across the gap between the two electrodes creates a spark. The spark-produced N wave propagates across the turbulent field of a plane jet. A wide-band condenser microphone picks up the signal. A centrifugal fan blows the air into the settling chamber. The air exits through the narrow slit and forms a plane jet. A detailed description is presented in Ref. [2].

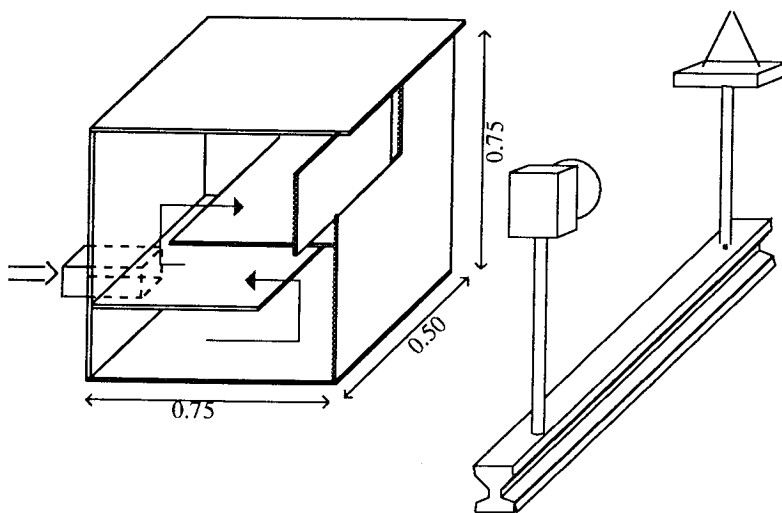


Figure 2: Model experiment setup.

In Fig. 3 several waveforms of the model experiment are shown. The upper left graph presents the waveform in absence of turbulence. All other waves have propagated through the turbulence. The distortion observed in the waveforms is very similar to that in sonic boom signatures, see e.g., [4]. Rounded and peaked waveforms are shown, as well as double and triple peaked waveforms.

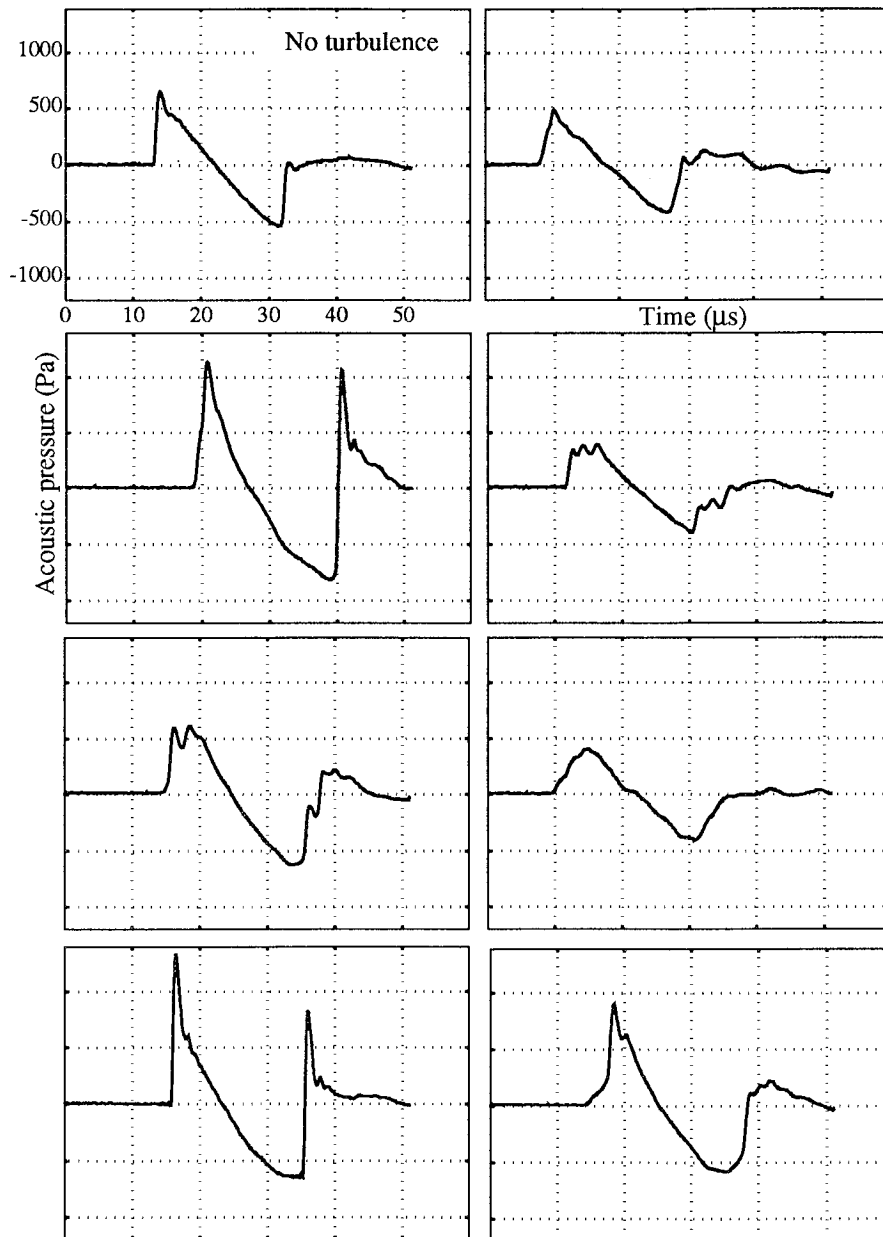


Figure 3: Waveform examples of the model experiment.

NONLINEAR PROPAGATION MODEL

We developed a model that simulates the weakly nonlinear acoustic propagation through turbulence. The main assumptions are: (1) linear geometric acoustics is sufficient to propagate the waves through the turbulent fields and (2) a nonlinear transport equation governs the propagation along the rays. We assume that the turbulence is frozen during passage of the wave. Thus, we model the turbulent medium as a set of independent realizations of a random field. The turbulent field of each realization is constructed as a sum of a finite number of Fourier modes. The model is flexible. Two-dimensional (2D) or three-dimensional (3D), scalar (e.g., temperature) or vectorial (e.g., velocity) fields can be constructed. The acoustic propagation model then consists of two parts. First, linear geometric acoustics is used to trace rays through each individual realization of the turbulent field. Then, a Pestorius' type algorithm [4] is used to solve numerically the nonlinear propagation equation along the rays.

Nonlinear Propagation Model

- assumptions: - linear geometric acoustics is used to trace rays
- nonlinear transport equation along the rays
- turbulence model: - 2D or 3D, temperature or velocity turbulence
- realizations constructed as a sum of discrete Fourier modes
- ray tracing through each realization of the turbulence
- nonlinear transport equation: - transformation into Burgers equation
- solved by a Pestorius type algorithm

Figure 4: Nonlinear propagation model.

TURBULENCE MODEL

The turbulent field is homogeneous and isotropic with a zero mean value. In Eq. 1 the construction of a turbulent velocity field as a sum of N modes is shown [6]. The direction of the turbulent wave vector \vec{K}^i of each mode is random and determined by the random angle θ_i (in 2D) (Fig. 5). The homogeneity of the turbulent field is assured by the random phase shift ϕ_i . The amplitude of each mode is determined by a predefined energy spectrum. For the results reported here a Gaussian longitudinal correlation function was assumed. The associated energy spectrum is shown in Fig. 6.

Turbulence model

$$\vec{v}'(\vec{x}) = \sum_1^N \vec{u}_i(\vec{K}^i) \cos(\vec{K}^i \cdot \vec{x} + \phi_i) \quad (1)$$

$$\vec{u}_i(\vec{K}^i) \cdot \vec{K}^i = 0$$

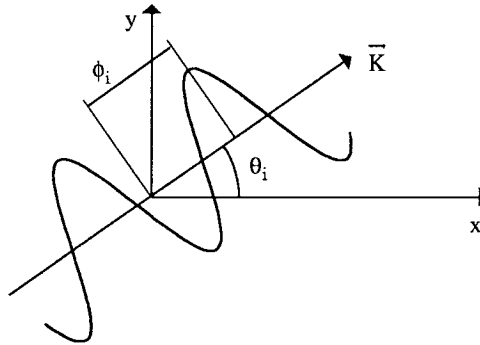


Figure 5: Wave vector geometry of a single Fourier velocity mode in 2D.

Two-dimensional kinetic energy spectrum

Gaussian longitudinal correlation function $f(r) = \exp(-r^2/L^2)$

Two-dimensional energy spectrum $E(K) = \frac{v'^2}{8} K^3 L^4 \exp(-K^2 L^2/4)$

Amplitude of each Fourier mode $|\vec{u}_i| = \sqrt{E(K) \Delta K}$

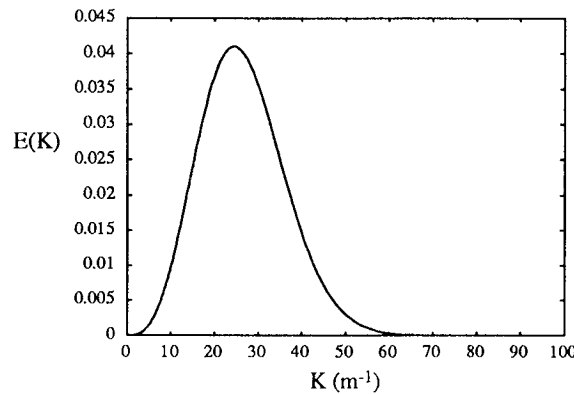


Figure 6: 2D energy spectrum for a Gaussian correlation function.

LINEAR GEOMETRIC ACOUSTICS

Equations 2–5 present the well-known formulation of acoustic propagation in the geometric acoustics limit [7]. The position vector \vec{x} (Eq. 2) and the nondimensional wave vector \vec{p} (Eq. 3) at a current point on the ray trajectory are completely determined by the value of s and the initial position along the incident wavefront. The local geodesic elements (Eqs. 4–5) govern the evolution of the wavefront along each ray and permit the calculation of the cross-sectional area of an infinitesimal ray tube. The parameters θ_0 and α_0 characterize the initial wavefront. The effect of the random field is represented by the index $N = c_0/c$ of the medium and the Mach number $\vec{M} = \vec{v}/c$ of the turbulent flow. Once initial conditions are known, a Runge–Kutta fourth-order scheme is used to solve the differential system. The step size ds is a function of the maximum wave number value of the turbulent energy spectrum, and equals $ds = 1/2k_{\max}$. It is important to note that the description of the turbulent field in terms of Fourier modes allows us to obtain analytically all the spatial derivatives in the system. Numerical errors are thus reduced.

Geometrical acoustics: Ray path equations

$$\frac{d\vec{x}}{ds} = \frac{1}{N}(\vec{v} + \vec{M}) \quad (2)$$

$$\frac{d\vec{p}}{ds} = \frac{1}{N}(\nabla N - (\nabla \vec{M}) \cdot \vec{p}) \quad (3)$$

$$\frac{d\vec{R}}{ds} = \frac{1}{pN}(\vec{Q} - \vec{v} \cdot \vec{Q}\vec{v}) \quad (4)$$

$$\begin{aligned} \frac{d\vec{Q}}{ds} = & \frac{1}{N}(\vec{R} \cdot \nabla \nabla N - \vec{R} \cdot (\nabla \nabla \vec{M}) \cdot \vec{p} - (\nabla \vec{M}) \cdot \vec{Q}) \\ & - \frac{1}{N^2}(\vec{R} \cdot \nabla N)(\nabla N - (\nabla \vec{M}) \cdot \vec{p}) \end{aligned} \quad (5)$$

where:

N is the index of the medium, i. e. $N = c_0/c$

$\vec{M} = \vec{v}/c$ is the Mach number vector, and \vec{v} is the fluid velocity vector
 \vec{x} is the vector describing the ray path

\vec{v} is the unit vector tangent to the ray path, i. e. $\vec{v} = \vec{p}/p$ and $\vec{p} = \vec{k}/k_0$

\vec{k} is the wavenumber vector and $k_0 = \omega/c_0$

\vec{R} is the vector describing the local geodesic elements of the wavefront, i. e. $\vec{R}^\theta = (\partial \vec{x} / \partial \theta_0)_{\alpha_0}$ and

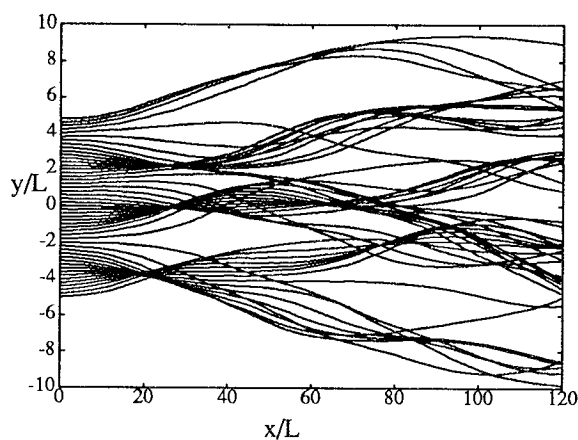
$\vec{R}^\alpha = (\partial \vec{x} / \partial \alpha_0)_{\theta_0}$

\vec{Q} are the conjugate elements of \vec{R}

In Fig. 7 two typical examples of ray-tracing through a random field are shown. The upper graph presents an example of a random temperature field with a scale of $L = 0.1$ m. During the first correlation lengths the rays are only slightly distorted and the initial plane wave structure is still apparent. At greater propagation distances the deflection of the rays is more pronounced, neighboring rays begin to cross, strong concentrations occur at different lateral positions, and caustics appear. The lower graph shows the propagation through a random velocity field. The length scale is the same, and the index fluctuations for the scalar and vectorial fields are identical, i.e., $\epsilon = -T'/2T_0 = -v'_x/c_0$, where T' is the rms temperature fluctuation and v'_x is the velocity fluctuation component in the propagation direction. The ray distortion for the velocity field is stronger than for the scalar field. The distance of caustics formation is shorter than for the scalar field.

Ray tracing through a single realization of a 2D isotropic scalar field

$$L = 0.1 \text{ m} \quad T'/2 T_0 = 5.882 \cdot 10^{-3}$$



Single realization of a 2D isotropic vectorial field

$$L = 0.1 \text{ m} \quad v'_x / c_0 = 5.882 \cdot 10^{-3}$$

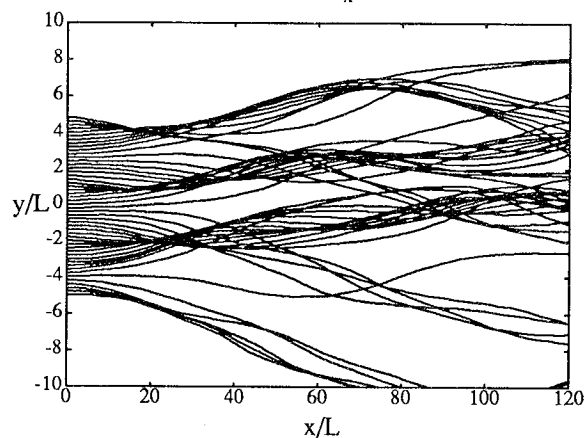


Figure 7: Examples of ray-tracing through a random temperature and velocity field.

NONLINEAR TRANSPORT EQUATION

The main assumptions in the derivation of the nonlinear transport equation are: (1) only quasi-linear terms are retained in the derivation, (2) lossless propagation is assumed, and (3) the geometric acoustics approximation is applied. Using the assumptions, we derive a transport equation (Eq. 6), where s represents the arclength along the ray, β is the coefficient of nonlinearity, t' is the retarded time coordinate, and A is the cross-section of the ray tube. Through a transformation of the dependent and independent variable the transport equation takes the form of the Burgers equation (Eq. 9) for plane wave propagation in a homogeneous medium. The distortion distance variable Z describes the equivalent plane wave distortion for a wave propagating in a random medium. Equation 8 is integrated numerically along the rays and yields the equivalent distortion value. The Burgers equation (Eq. 9) is solved numerically by a Pestorius' type algorithm [5]. The nonlinear distortion is applied in the time domain and an ad-hoc absorption is applied in the frequency domain.

Nonlinear transport equation:

Main assumptions: - quasi-linear
 - lossless
 - geometric acoustics approximation

$$\frac{\partial}{\partial s} \left[\frac{p^2 |A|}{c \rho_0} (1 + \vec{v} \cdot \vec{M}) |\vec{v} + \vec{M}| \right] - \frac{2\beta |A|}{\rho_0^2 c_0^4} p^2 p_{t'} = 0 \quad (6)$$

Transformation of the dependent and independent variable

Let $\Pi = Kp$, where

$$K = \sqrt{\frac{|A|}{|A_0|} \frac{\rho_0 c_0}{\rho c} (1 + \vec{v} \cdot \vec{M}) |\vec{v} + \vec{M}|} \quad (7)$$

and

$$\frac{dZ}{ds} = \sqrt{\frac{|A_0|}{|A|} \frac{\beta^2 \rho_0 c_0^5}{\beta_0^2 \rho c^5} (1 + \vec{v} \cdot \vec{M})^{-3} |\vec{v} + \vec{M}|^{-3}} \quad (8)$$

The transport equation is transformed into the homogeneous plane wave Burgers equation

$$\frac{\partial \Pi}{\partial Z} - \frac{\beta_0}{\rho_0 c_0^3} \Pi \Pi_{t'} = 0 \quad (9)$$

COMPUTATION STRATEGY

The computation strategy involves the following steps. First, individual realizations of the turbulent field are constructed. Second, eigenrays that connect source and receiver are computed, and the properties K and Z are calculated along the eigenrays. Third, a Pestorius' type algorithm is used to propagate a given waveform nonlinearly along the eigenrays. Finally, the waveforms associated with all eigenrays are combined to obtain the signal at the receiver. If a waveform passes through a caustic, the propagation proceeds up to the caustic, then a -90° phase shift is applied in the frequency domain, and propagation proceeds again.

Strategy

- create realizations of turbulent field
- compute eigenrays and properties (K, Z) along the eigenrays
- use Pestorius algorithm to propagate a waveform nonlinearly along the eigenrays
- combine eigenrays to obtain signal at the receiver
- if waveform passes through a caustic, propagation proceeds up to the caustic, then a -90° phase shift is applied in the frequency domain, and propagation continues

EXAMPLE OF EIGENRAY CALCULATION FOR ONE REALIZATION

The upper graph in Fig. 8 represents the 7 eigenrays that connect the initial plane wavefront with the receiver located at 8 m on the x-axis. The second graph shows the values of K along the rays. When the eigenray passes through a caustic, the value of K drops to zero, i.e., an infinite pressure, a consequence of the linear geometric acoustics assumption. As is observed, one eigenray passed through two caustics, three rays passed through one caustic, and three rays did not yet pass through a caustic. The third graph presents the equivalent plane wave distortion distance Z . For the ray that passed through two caustics, the equivalent distortion distance is nearly 14 m when the actual propagation distance to the receiver is about 8 m. Thus, the nonlinear distortion along this ray is equivalent to that of a plane wave that propagated about 14 m in a homogeneous medium. For one ray that did not propagate through a caustic, the equivalent distortion distance is just slightly more than 2 m, and hence the nonlinear distortion will be very weak compared to the homogeneous case.

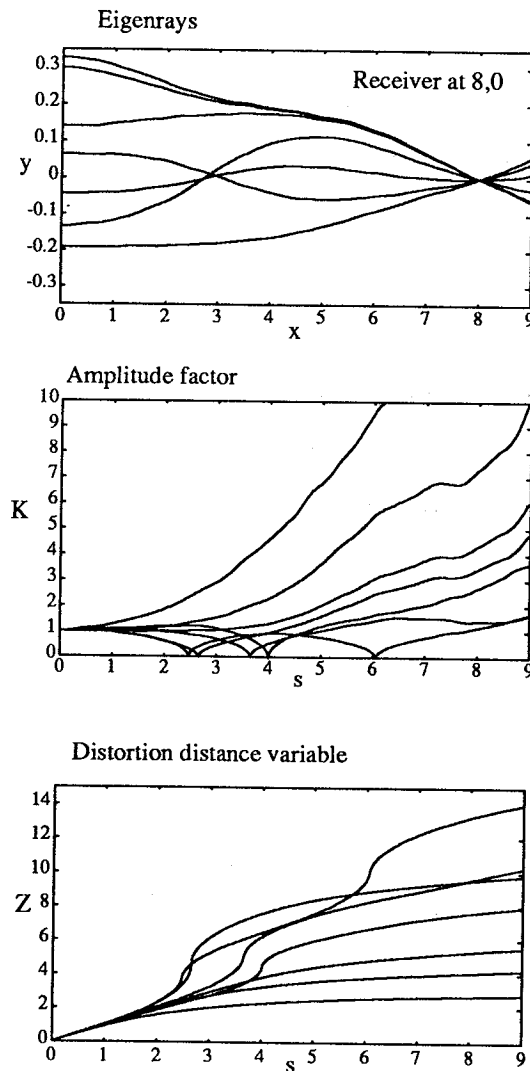


Figure 8: Examples of eigenray and associated K and Z calculation.

PARAMETERS FOR THE NUMERICAL STUDY

The parameters for the numerical experiment are shown in Fig. 9. Both temperature and velocity turbulent fields are constructed. Both fields have a length scale of $L = 2.5$ cm. The index of fluctuations ϵ is identical for both fields. The rms velocity fluctuation is 2.5 m/s and the rms temperature fluctuation is 4.27 K. Each realization is constructed as a sum of 60 Fourier modes equally divided between a lower wave number value of $0.1 L$ and an upper value of $10 L$. Statistics are calculated for an ensemble of 100 realizations. The incident acoustic wave is a plane N wave of peak pressure 500 Pa, duration 15 μ s, and rise time 1 μ s. The propagation medium is air, and classical thermo-viscous absorption is included in the Pestorius' algorithm as well as O_2 and N_2 relaxation.

Parameters for numerical study

- Turbulence: 60 modes between 0.1 L and 10 L

$$L = 2.5 \text{ cm}$$

$$v' = 2.5 \text{ m/s and } T' = 4.27 \text{ K}$$

100 realizations

- plane N wave: 500 Pa peak pressure

15 μ s duration

1 μ s rise time

- medium: classical absorption

O_2 and N_2 relaxation

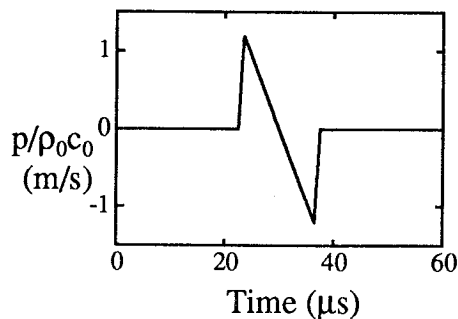


Figure 9: Parameters for the numerical study.

AVERAGED RESULTS FOR THE PARAMETERS Z AND K

In the upper graph of Fig. 10 the value of Z averaged over 100 realizations is shown. Three curves are presented, i.e., for the no turbulence, temperature turbulence, and velocity turbulence case. It is seen that the presence of turbulence always results in a lower value for the equivalent distortion distance. The effect is more pronounced when propagation distance increases, and stronger for the velocity turbulence. At a propagation distance of 2 m the equivalent distortion distance for the velocity turbulence is slightly more than 50% that of the no turbulence case. The lower graph presents the values of the amplitude factor K . The factor increases rapidly with propagation distance, and the effect is more pronounced for the velocity turbulence.

Results for Z and K parameters

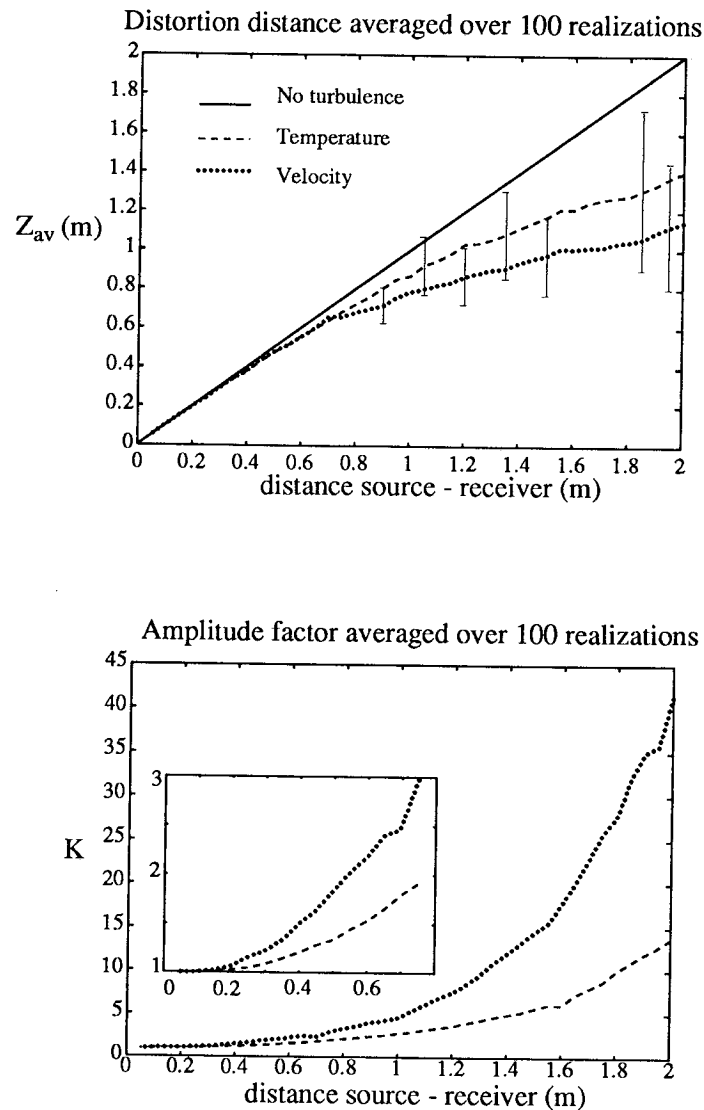


Figure 10: Averaged results for parameters Z and K .

EXAMPLE OF WAVEFORM CALCULATION

An example of a waveform calculation is shown in Fig. 11. The total waveform at the receiver is shown in the upper graph. For this particular example 5 eigenrays exist. The lower graph presents the contribution of the waveform of each eigenray to the total signal. Two waves have passed through a caustic, and the other three have not passed through a caustic. The latter three arrive at the receiver at nearly the same time and are hard to distinguish.

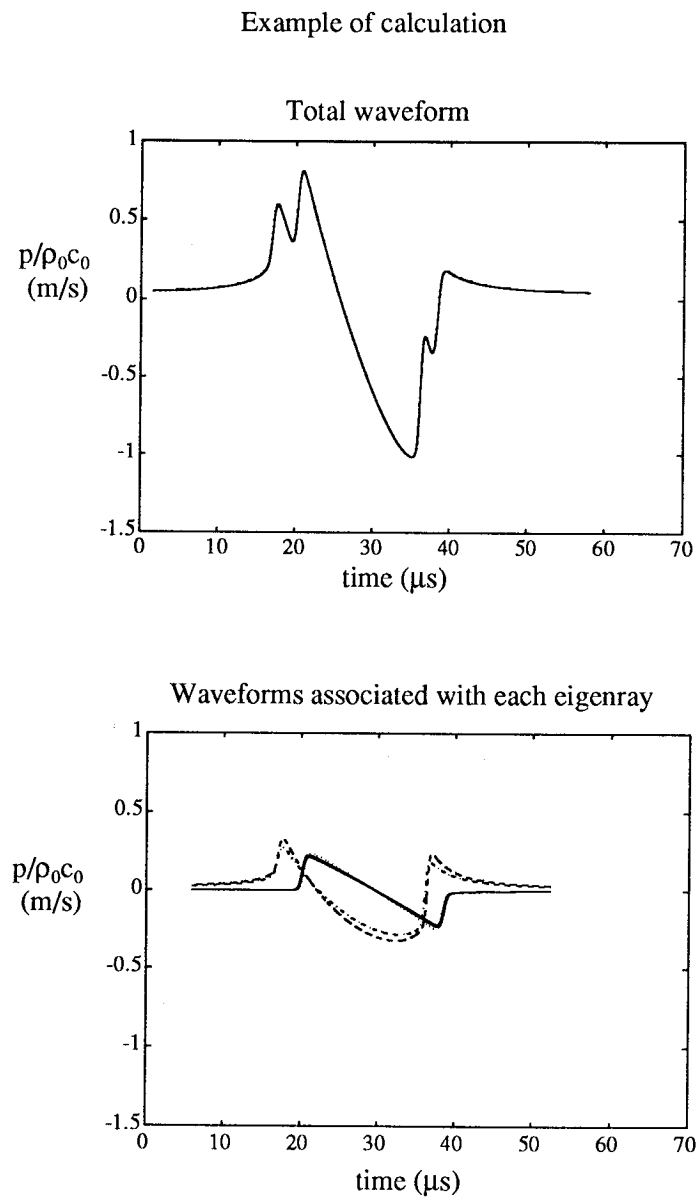


Figure 11: Example of waveform calculation.

WAVEFORM EXAMPLES

In Fig. 12 several examples of waveforms calculated at the receiver at a distance of $18L$ or $20L$ are shown. The upper left graph presents the waveform at a distance of $18L$ in absence of turbulence. All other waves have propagated through a turbulent field. In general the distortion of the waveform is similar to that measured in spark-produced N waves (Fig. 3).

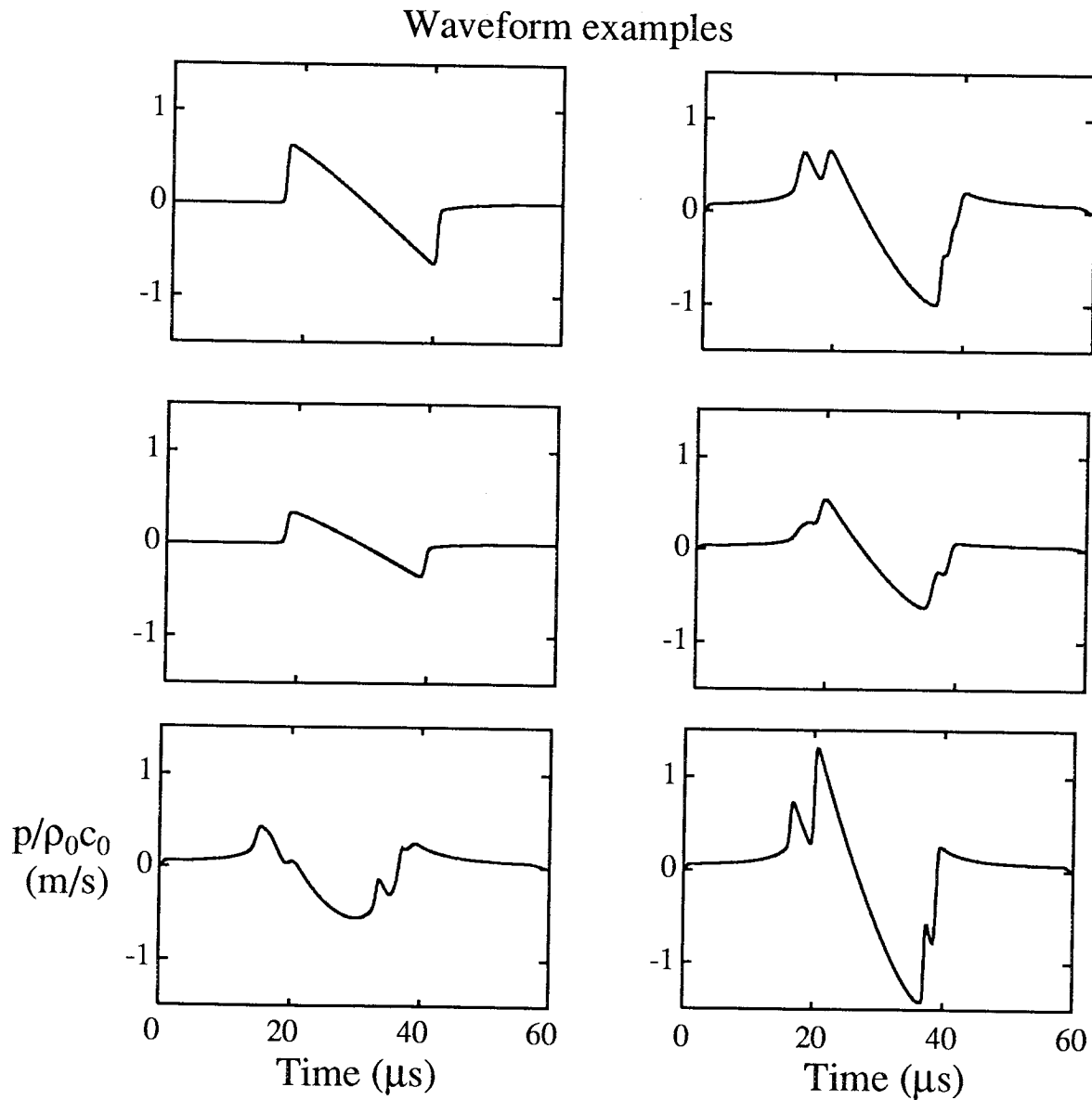


Figure 12: Waveform examples.

RESULTS FOR THE TOTAL WAVEFORM AT THE RECEIVER

The average values of peak pressure and rise time of the total waveform calculated at different receiver distances are shown in Fig. 13. The rise time is calculated as the time portion between 10% and 90% of the peak pressure of the total waveform. According to this definition, we notice that the rise time is essentially determined by the differences in arrival time of the eigenrays when more than one eigenray is present (see, e.g., Fig. 11). The average is taken over 100 realizations. In the presence of turbulence, peak pressure is always decreased. There is no notable difference between the temperature and velocity turbulence. At a distance of 1 m a decrease of about 25% is observed. This result confirms the model experiment results [3] that peak pressure on average is always decreased by turbulence. The lower graph presents the average value of rise time. On average, rise time is always increased by turbulence. At a propagation distance of 1 m, a tenfold increase is observed. Again, this result confirms that of the model experiment. The effect is more pronounced for the velocity fields. The curves start to deviate from the no turbulence case when the rays pass through the first caustic. The shorter distance to the first caustic for the velocity fields explains the quicker departure from the no turbulence values.

Results for total waveform at the receiver

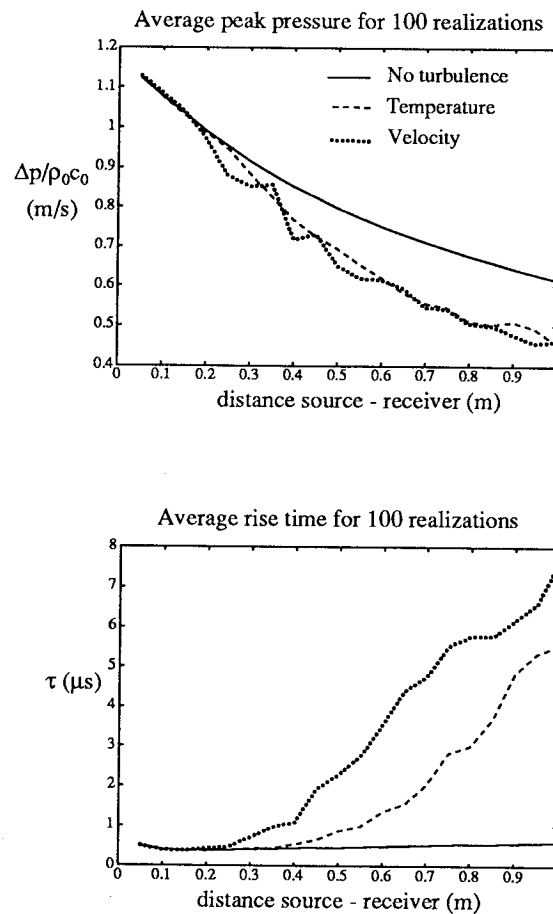


Figure 13: Average values of peak pressure and rise time of the total waveform for 100 realizations.

HISTOGRAMS OF PEAK PRESSURE AND RISE TIME

The histograms of peak pressure and rise time at different distances of propagation are shown in Fig. 14. The thick black vertical line in each graph represents the value for the plane wave case in absence of turbulence. The distribution for the peak pressure is asymmetric. Peak pressures smaller than the no turbulence value occur more often, but some large values of peak pressure are always present. The rise time histograms show that turbulence almost always causes the rise time to increase. When propagation distance increases, larger values for the rise time occur once the rays have passed through the first caustic (e.g., at a distance of $20 L$). When rays pass through several caustics, rise times more than 20 times that of the no turbulence value are observed (e.g., at $40 L$).

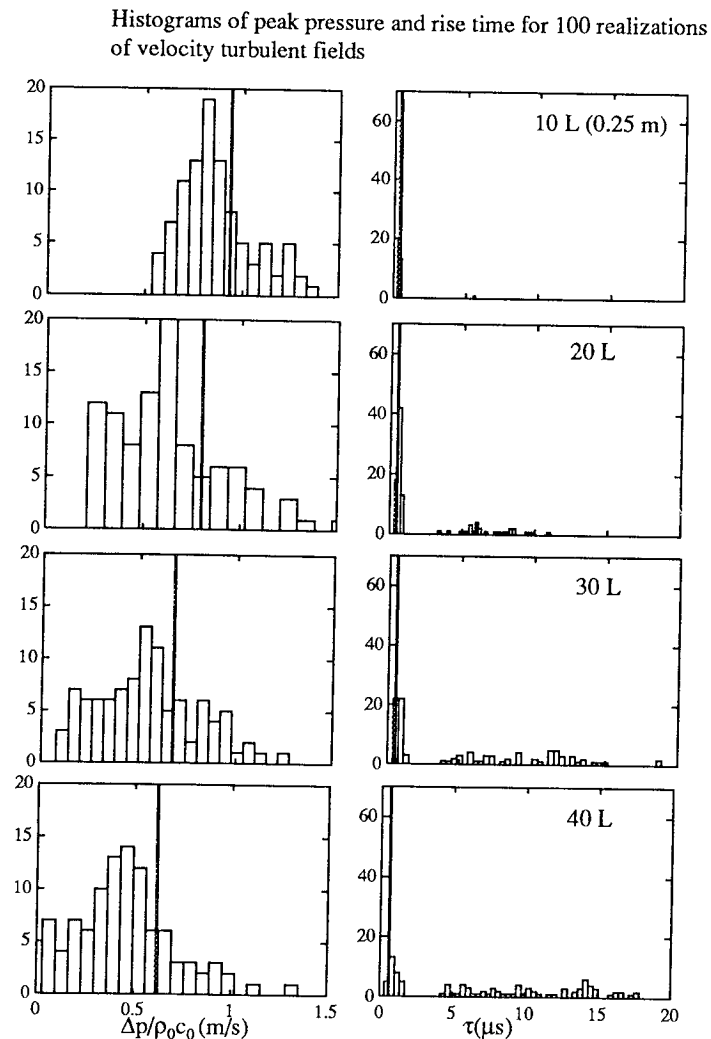


Figure 14: Histograms of peak pressure and rise time for 100 realizations.

RESULTS FOR THE INDIVIDUAL WAVEFORMS ASSOCIATED WITH EACH EIGENRAY

A second statistical calculation is performed. In order to filter out the effect of the difference in arrival time for all the eigenrays, we calculated the peak pressure and rise time of the individual waveforms associated with each eigenray. The waveform shown in Fig. 11 consists of 5 eigenrays. Instead of calculating the peak pressure and rise time of the global waveform, we calculate the peak pressure and rise time of the three waveforms that have not yet passed through a caustic. We do not take into account the rays that have passed through a caustic because the 10% to 90% criterion results in very large values. A better criterion for these waveforms would be a rise time value based on a maximum slope value. The result of the calculation is shown in Fig. 15. The average peak pressure is again always decreased by turbulence. Average peak pressure for velocity turbulence is lower than that for the temperature turbulence. The average rise time values are always increased by the turbulence. The difference is less marked when compared with the previous calculation. For the velocity turbulence a doubling of the rise time is observed at a propagation distance of 1 m. Again the effect is more pronounced for the velocity fields. The slope of the rise time versus distance curve is linear. The larger slope for the velocity fields is caused by the vectorial character of the fields.

Results for individual contributions of each eigenray

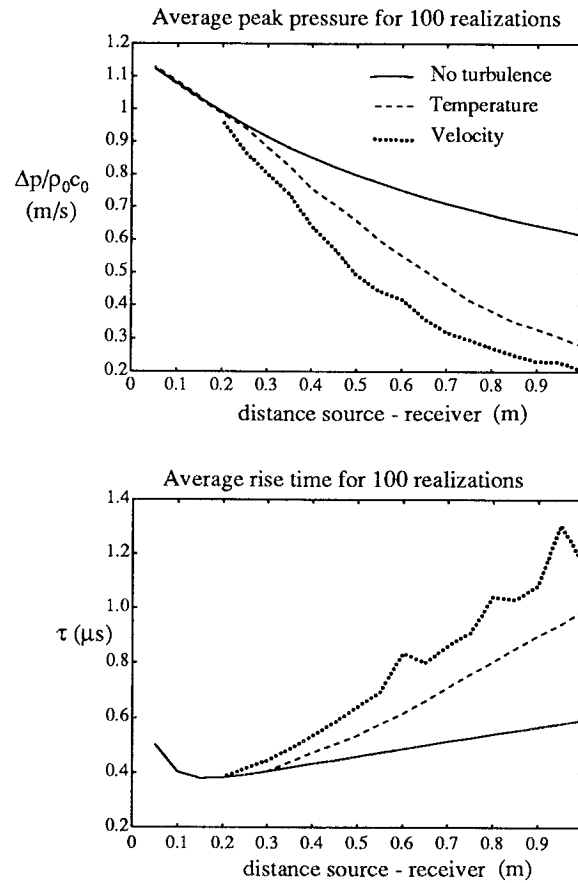


Figure 15: Average values of peak pressure and rise time of the waveforms associated with the eigenrays.

CONCLUSIONS

We presented a model for the nonlinear propagation of sonic booms and spark-produced N waves through turbulence. A numerical experiment that simulates the propagation of spark-produced N waves through 2D temperature and velocity turbulent fields was performed. The results from the numerical experiment confirm the experimental observations of the model experiment in which spark-produced N waves propagated through a plane jet turbulence. An important conclusion is that the presence of turbulence on average reduces the nonlinear distortion. It is however possible that for a particular realization the nonlinear distortion is stronger. On average, peak pressure is always decreased by turbulence. Turbulence almost always causes the rise time to increase. The computed waveforms show similar distortion as that obtained in the model experiment. The effect of turbulent velocity fields is more pronounced than that of temperature fields and is caused by the difference in character, i.e., vectorial for the velocity fields versus scalar for the temperature fields. Future work includes a calculation with a more realistic turbulent energy spectrum and the incorporation of boundaries.

Conclusions

- Model presented for the nonlinear acoustic propagation through turbulence.
- On average, turbulence reduces the nonlinear distortion.
- On average, peak pressure decreases after propagation through turbulence.
- Rise time is almost always increased by turbulence.
- Effect of velocity turbulence is more pronounced than that of thermal turbulence.

Figure 16: Conclusions.

References

- [1] A. Niedzwiecki and H. S. Ribner, "Subjective loudness of N-wave sonic booms," *J. Acoust. Soc. Am.* **64**, 1622-1626 (1978).
- [2] J. D. Leatherwood and B. M. Sullivan, "Subjective loudness response to simulated sonic booms," Proceedings, High-Speed Research Workshop on Sonic Boom, NASA Langley Research Center, Hampton, Virginia, C. M. Darden, ed., Vol. I, pp. 151-170 (1992).
- [3] B. Lipkens, "Experimental and theoretical study of the propagation of N waves through a turbulent medium," Ph. D. dissertation, Department of Mechanical Engineering, University of Texas at Austin (1993).
- [4] R. A. Lee and J. M. Downing, "Sonic boom produced by United States Air Force and United States Navy aircraft: measured data," AL-TR-1991-0099, Armstrong Laboratory, Wright-Patterson Air Force Base, Ohio (1991).
- [5] F. M. Pestorius, "Propagation of plane acoustic noise of finite amplitude," ARL Technical Report No. 73-23, Applied Research Laboratories, The University of Texas at Austin (AD 778868) (1973).
- [6] Ph. Blanc-Benon, *et al.*, "Occurrence of caustics for high-frequency acoustic waves propagating through turbulent fields," *Theoret. Comput. Fluid Dynamics* (1991) 2:271-278.
- [7] S. M. Candel, "Numerical solution of conservation equations arising in linear wave theory: application to aeroacoustics," *J. Fluid Mech.* **83**, 465-493 (1977).